Journal Syifa Sciences and Clinical Research (JSSCR)
Volume 8 Nomor 1, 2026
Journal Homepage: http://ejurnal.ung.ac.id/index.php/jsscr, E-ISSN: 2656-9612 P-ISSN:2656-8187
DOI : https://doi.org/10.37311/jsscr.v8i1.33360

In Silico Screening of Annona Metabolites Against CYP17A1 and β-tubulin Using PLANTS Docking

Didik Rio Pambudi[1], Hafiz Ramadhan[2*], Citra Kharisma Dewi[3]

[1,2,3] *Faculty of Pharmacy, University of Borneo Lestari,*
Jl. Kelapa Sawit 8 Bumi Berkat, Banjarbaru 70714, Indonesia

** Corresponding author Email: hafizramadhan14@gmail.com*

ABSTRACT

Prostate cancer progression is closely associated with androgen biosynthesis mediated by cytochrome P450 17A1 (CYP17A1) and with microtubule dynamics regulated by β-tubulin, making both proteins important therapeutic targets. The Annona genus is a rich source of acetogenins with reported anticancer potential; however, their interactions with prostate cancer–related targets remain insufficiently explored. In this study, an in silico exploratory approach was employed to evaluate 30 Annona-derived compounds against CYP17A1 (PDB ID: 3RUK) and β-tubulin (PDB ID: 1JFF) using the PLANTS (v1.1) molecular docking program. Docking protocol validation was based on RMSD values ≤ 2 Å, and compound prioritization was performed using docking scores and binding-site residue similarity relative to native ligands and reference drugs. The docking results identified squafosacin-C as the top-ranked compound for both targets, exhibiting docking scores of −133.289 for CYP17A1 and −131.825 for β-tubulin. These values were more favorable than those of the native ligands (−82.5591 and −103.071) and the reference drugs abiraterone and docetaxel (−83.6465 and −99.7319, respectively). Visualization analysis further revealed that squafosacin-C shares 7 of 8 key amino acid residues involved in native ligand binding at both targets, indicating a conserved binding mode. In conclusion, based on molecular docking and interaction analysis, squafosacin-C emerges as a promising lead compound at the computational level for targeting CYP17A1 and β-tubulin in prostate cancer. These findings provide a rationale for further investigation through molecular dynamics simulations and experimental validation to confirm its biological activity.

Keywords:
Molecuular docking; PLANTS; Prostate cancer; Annona; Acetogenins

Received:	*Accepted:*	*Online:*
2025-07-10	*2026-02-19*	*2026-03-01*

1. Introduction

Cancer is a disease caused by the uncontrolled growth of abnormal cells in the body, whereby the cells divide rapidly, causing damage to healthy tissues and potentially spreading to other parts of the body (metastasis). In 2020, prostate cancer ranked as the second most prevalent cancer (14.1%) and the fifth leading cause of cancer-related deaths (6.8%) among men [1]. Prostate cancer is a malignancy that develops within the male reproductive system. Most prostate cancers initially arise from the cells lining the prostate gland and are referred to as prostate adenocarcinoma, which is characterised by glandular formation and the expression of luminal differentiation markers such as androgen receptor (AR) and prostate-specific antigen (PSA). To date, the exact cause of prostate cancer remains unknown; however, several risk factors have

been associated with its development and progression. These include age over 40, family history, and unhealthy lifestyle choices [2].

One of the key enzymes in steroidogenesis is CYP17A1 (Cytochrome P450 17A1). This enzyme has dual activity as a 17α-hydroxylase and 17,20-lyase, converting pregnenolone and progesterone into precursors for testosterone and dihydrotestosterone (DHT) [3]. CYP17A1 is a key enzyme in neurosteroid-driven steroid biosynthesis, playing a vital role in maintaining brain homeostasis and contributing to the development of prostate cancer [4]. Inhibition of CYP17A1 has been clinically shown (for example, through the use of Abiraterone) to extend patient survival; however, drug resistance often arises through point mutations or alternative pathways. On the other hand, the standard chemotherapy strategy for metastatic prostate cancer often involves microtubule-disrupting agents, such as the taxane class (Docetaxel and Cabazitaxel). These drugs work by binding to beta-tubulin (β-tubulin), which leads to stabilization or destabilization of microtubule polymerization because the increased expression of β-tubulin in advanced prostate cancer is linked to neuroendocrine transdifferentiation, a process associated with tumor progression. Agents that attach to specific β-tubulin domains induce microtubule depolymerization in prostate cancer by suppressing microtubule assembly and dismantling the cytoskeletal structure, which triggers cell cycle arrest at the G2/M phase and induces apoptosis. Interestingly, there is a mechanistic link between microtubule integrity and androgen receptor nuclear trafficking; disruption of β-tubulin not only halts mitosis but also inhibits AR translocation into the cell nucleus, thereby suppressing the transcription of androgen target genes [5],[6].

Although docetaxel-based chemotherapy, which stabilizes microtubules, remains the standard treatment for castration-resistant prostate cancer, microtubule-disrupting agents—such as Vinca alkaloids, estramustine, and colchicine-binding compounds—play an important role in circumventing therapeutic resistance and suppressing androgen receptor (AR) signaling [7]. These microtubule-targeting agents (MTAs) are widely applied in oncology; however, their clinical use is limited by considerable drawbacks, including systemic toxicity, the emergence of drug resistance, and unfavorable pharmacokinetic properties. Although effective at blocking mitosis, their poor selectivity between malignant cells and rapidly proliferating normal tissues leads to severe dose-limiting adverse effects [8]. Consequently, continued investigation is required to address these challenges, particularly through the development of safer and more natural-based therapeutic options for prostate cancer.

The genus Annona (Annonaceae), which is rich in Annonaceous Acetogenins (AGEs), has hypothetically attracted considerable attention due to its potent bioactivity as a cytotoxic agent against various cancer cell lines; however, its mechanisms against specific targets such as CYP17A1 and microtubules in prostate cancer still require further investigation [9]. One approach that can be utilised to identify potential compounds as anticancer agents is in silico testing. In silico studies serve as preliminary methods in the discovery of new drug candidates and contribute to the optimisation of compounds in the healthcare field. Moreover, in silico studies can be used to explore natural compounds targeting specific proteins [5]. Therefore, this study we screened 30 Annona metabolites against CYP17A1 (3RUK) and β-tubulin (1JFF) with PLANTS, validated docking by redocking RMSD (≤2 Å), ranked candidates by score and residue-match to co-crystallized ligands, and assessed oral drug-likeness.

2. Methods

Equipment and Materials

The tool used is an Acer Aspire 5 - 2DAJ1QPU specifications: Processor 11th Gen Intel(R) Core(TM) i5-1135G7 with NVIDIA GeForce Graphics 2.40 GHz, Intel Chipset, Graphic NVIDIA GeForce MX350 Graphics, 8GB RAM memory. Equipped with Windows 11 office Home system. Installed software used PubChem; Protein Data Bank (PDB); MarvinSketch v.5.2.5.1; ChemDraw v.12.0.2; YASARA v.10.1.8.; Discovery Studio Visualizer and to run docking using PLANTs® v1.1. The materials used are thirty compounds from the *Annona* genus, which were obtained and identified through a literature search. *Abiraterone* and *Docetaxel* as compound comparison drugs. Target proteins CYP17A1 (PDB ID: 3RUK) and β-tubulin (PDB ID: 1JFF) [9],[10].

Protein Structure Preparation

Proteins downloaded from the official website of the Protein Data Bank (www.rcsb.org) in "pdb" format need to be prepared using the YASARA application before performing the docking process. Then the protein structure is separated from the docking protocol (ions, water, ligands). During preparation of the CYP17A1 structure (PDB ID: 3RUK), chain A was chosen from the four available chains (A–D) associated with the native ligand abiraterone, and the HEM group (iron-containing protoporphyrin IX) was removed. For the 1JFF receptor, which represents the α/β-tubulin complex, chain B was selected to retain only the β-tubulin subunit, with all bound ligands removed except the native ligand Taxol. In addition, water molecules and ions associated with both receptors were eliminated during the preparation steps [11].

Ligand Preparation

The application used for the preparation of Native ligands, comparison compounds, and test compounds can be drawn using MarvinSketch. The ligand was created in the form of a 2D model and determined the protonation/tautomer state at pH 7.4, saved with the file name "ligand2D.mrv". It was then generated with "conformations" and saved as "ligand.mol2" to form a source of stereochemistry, and energy minimisation before docking. Procedures carried out in the docking protocol for native ligand, comparator compound, and test compound [11],[12].

Docking Validation

Docking validation against the original ligand was done to Find the confirmation of the original ligand. The target protein structure was docked with docking protocols ("ref_ligand.mol2" and "protein.mol2") that had previously been prepared using the PLANTs application to see the docking score of 3RUK and 1JFF target proteins. After that, calculate the RMSD (Root Mean Square Distance) value of the docking results using the YASARA program [11],[12].

Molecular Docking with PLANTS

Operate the PLANTS application, then perform docking on the "load" file native ligand, test compounds, and compounds comparison of the docking protocol that has been prepared before, by writing the "input script" on command prompt PLANTs until the output score docking is obtained as scoring function ChemPLP (Chemical Piecewise Linear Potential) value and speed 1 was set as search speed. The binding site is defined using a center point (XYZ coordinates) and a radius (in Ångströms, Å) that defines a sphere encompassing the active site. The command "plants --mode bind ligand.mol2 protein.mol2" can be used to automatically define the center and radius. Docking results from the configuration to output the top 10 poses can be seen in Excel format with the file name bestranking.csv in the docking protocol result folder. The score reflects the

affinity energy, while it is often treated as an arbitrary unit from a technical standpoint, it is commonly interpreted or transformed into kJ/mol as an estimate of binding free energy [11],[13],[14].

Visualization Lipinski Rule of Five Test

The purpose of molecular docking visualization is to see the interaction between ligands and amino acid residues in the receptor. The process involves selecting protein preparation in .pdb format and displaying the best conformation of docking results in 2D and 3D using a visualization-based program, Discovery Studio Visualizer [11],[13].

Lipinski Rule of Five Test

A compound is declared as a drug molecule if it has the ability to penetrate membranes in the digestive tract and cell membranes, and can effectively reach target proteins easily. A compound is considered a drug molecule if it does not violate more than one rule of Lipinski's Rule of Five (Lipinski's RO5). Drug-likeness was assessed using Lipinski's RO5 (MW ≤ 500 g/mol, LogP ≤ 5, H-bond donors ≤ 5, H-bond acceptors ≤ 10) and the Ghose filter (MW 160–480 g/mol, WlogP −0.4 to 5.6, total atoms 20–70, molar refractivity (MR) 40–130). MR is reported as a dimensionless descriptor as returned by SwissADME [15],[16].

3. Results and Discussion

Docking Validation

Docking validation was performed to evaluate the reliability of the docking protocol by redocking the native ligands into their respective binding sites and comparing the predicted poses with the crystallographic conformations, a standard approach in structure-based drug design studies [17],[18]. Method validity was assessed using the root mean square deviation (RMSD), with values below 2.0 Å generally accepted as indicative of accurate pose reproduction in molecular docking analyses [19],[20]. In this work, the best redocked pose of the CYP17A1 inhibitor in 3RUK yielded an RMSD of 0.5879 Å, while the optimal redocked pose of the β-tubulin ligand in 1JFF showed an RMSD of 1.5213 Å, confirming that the docking protocol can reliably reproduce the experimentally observed binding modes (**Table 1**).

Table 1. RMSD of Native ligand

Proteins	Conformation	Docking Score (KJ/mol)	RMSD
3RUK (Inhibitor CYP17A1)	1	-82.1984	0.5901
	2	-82.5591	0.5879
	3	-82.124	0.5956
	4	-82.4837	0.6011
	5	-81.4166	0.8644
	6	-81.4569	0.8714
	7	-81.4408	0.8622
	8	-81.5479	0.8221
	9	-81.4945	0.8555
	10	-81.7227	0.8335
1JFF (Receptor β-tubulin)	1	-90.1581	8.2314
	2	-93.5721	7.1973
	3	-101.195	7.0372
	4	-99.6875	7.4463

5	-100.474	1.5213
6	-103.071	6.6878
7	-95.7631	7.5823
8	-97.9717	2.6394
9	-99.1421	8.0155
10	-101.81	7.2781

Information:

The best value that satisfies the parameter RMSD < 2 Å

Superposition of the crystallographic and redocked ligands demonstrates a high degree of spatial overlap for both targets, particularly for 3RUK, where ligand orientation and key interaction geometry are well conserved, consistent with reliable docking performance [17]. For 1JFF, although one pose satisfies the RMSD < 2 Å criterion, several alternative redocking runs resulted in substantially larger RMSD values (≈7–8 Å). This deviation is attributable to the structural complexity of β-tubulin, which possesses an extended and flexible binding cavity with multiple ligand-accessible regions, allowing ligand placement outside the canonical taxane-binding pocket when spatial constraints are not applied [21].

To address this issue, docking calculations for 1JFF were restricted to the native ligand binding site defined by the crystallographic coordinates of the co-crystallized ligand, an approach commonly recommended for tubulin-targeted docking studies [20],[21]. Only poses generated within this constrained region were considered for validation and subsequent analysis, effectively excluding non-physiological binding modes and ensuring that the selected pose (RMSD = 1.5213 Å) reflects the experimentally relevant interaction site. Similar observations regarding elevated RMSD values in unconstrained tubulin docking and the necessity of binding-site definition have been reported in recent docking validation studies [18],[21].

Molecular Docking

Molecular docking remains a foundational in silico tool in early-stage drug discovery, enabling the rapid evaluation of ligand binding affinities against defined protein targets and offering structural insights that can guide experimental validation [22]. Within this framework, we independently assessed the binding interactions of compounds derived from Annona species against two clinically relevant prostate cancer protein targets: CYP17A1 (3RUK) and β-tubulin (1JFF). It is critical to emphasize that docking scores are target-specific and cannot be directly compared across receptors due to distinct binding site chemistries and scoring function sensitivities. More negative docking scores consistently reflect greater predicted binding affinity within each respective target (i.e., lower ΔG suggests stronger interactions) [23]. Molecular docking of compounds from the Annona genus was performed in the PLANTS application, through the docking process with the prepared protein targets (3RUK and 1JFF). 3RUK works to significantly reduce intracellular testosterone by suppressing its synthesis in both the adrenal glands and cancer cells. Whereas 1JFF works by disrupting the assembly of microtubules from tubulin dimers and preventing depolymerization of tubulin, thus stabilizing microtubules in cells while inhibiting DNA, RNA, and protein synthesis, with its main activity occurring during the M phase of the cell cycle [24],[25].

Cytochrome P450 17A1 (CYP17A1) is a key enzyme in androgen biosynthesis, functioning at a rate-limiting step that underpins prostate cancer progression and castration-resistant disease. Inhibitors such as abiraterone acetate, approved for

metastatic castration-resistant prostate cancer, exploit direct binding to the CYP17A1 active site to suppress androgen synthesis, thereby attenuating tumor growth (structurally and functionally explored in docking and dynamics studies) [26. Against CYP17A1 (3RUK), our docking analysis indicated that all evaluated Annona compounds marked with green color (**Table 2**) exhibited more negative binding scores than both the native ligand (−82.5591) and the comparator drug abiraterone (−83.6465), supporting enhanced predicted affinity within this target. Notably, acetogenins such as Squafosacin-C (−133.289), Muricin A (−129.741), Cis-annonacin (−129.145), Annomolin (-128.425), and Annomuricine E (-125.936) consistently populated the top of the ranking list (Table 2), indicating a strong propensity for active site engagement.

To aid interpretability and reproducibility, we present these results in **Table 2**, which includes docking score (ΔG), **Figure 1** shows key interacting residues within the CYP17A1 binding pocket, and **Table 3** employs hydrogen and/or non-hydrogen bond types. This structured presentation ensures clarity in how each ligand engages the heme-proximal active site and adjacent hydrophobic residues, facilitating mechanistic comparisons with known inhibitors. Additionally, including interaction distances contextualizes how hydrogen bonds complement hydrophobic contacts to strengthen binding—a principle supported by recent in silico studies on natural product docking to CYP17A1 targets [27].

On the other hand, β-Tubulin represents a validated anticancer target due to its central role in microtubule dynamics and cell division. Many chemotherapeutics (e.g., taxanes, vinca alkaloids) exert efficacy through tubulin binding that disrupts polymerization, leading to mitotic arrest and apoptosis. Although binding sites differ among tubulin inhibitors, in silico docking has been widely applied to predict ligand interactions and guide analogue design in tubulin inhibitor development (as seen in recent studies exploring quinoline and stilbene derivatives) [28]. Our docking against β-tubulin (1JFF) similarly showed that five Annona compounds, particularly Squafosacin-C (−131.825), Annomolin (−126.988), Muricin A (−124.038), Cis-annonacin (-122.669), and Annomuricine E (-121.313), exhibited more negative binding scores than both the native ligand (−103.071) and the reference drug docetaxel (−99.7319). This suggests stronger predicted binding within the colchicine or taxane pocket regions of β-tubulin. Accordingly, we also provide detailed docking scores in **Table 2**, interacting residues relevant to microtubule binding in **Figure 2**, and the type of bond formed in **Table 4**. Such information is essential for elucidating putative binding modes and for rationalizing ligand effects on microtubule polymerization in subsequent experimental validation.

Integrating these target-specific profiles, several Annona compounds, including Annomolin, Cis-annonacin, Annomuricine E, Squafosacin-C, and Muricin A, were among the top scorers in both CYP17A1 and β-tubulin docking analyses. Within the constraints of in silico modeling, this suggests a multitarget binding potential that could be exploited in polypharmacological strategies against prostate cancer. However, it is essential to interpret these results in light of known biochemical constraints: docking scores are predictive and do not inherently measure biological efficacy or selectivity, and further in vitro and in vivo validation is required to confirm therapeutic potential.

Table 2. Docking scores of *Annona* genus compounds against 3RUK and 1JFF proteins

No	Compounds	Docking Score (KJ/mol)	
		3RUK	1JFF
1	*Native Ligand*	-82.5591	-103.071
2	*Abiraterone* (Comparator drug)	-83.6465	-
3	*Docetaxel* (Comparator drug)	-	-99.7319
4	*Anomuricine*	-83.7953	-70.6544
5	*Anomurine*	-81.6643	-70.6388
6	*Anonaine*	-75.9698	-70.3771
7	*Asimilobine*	-73.1247	-66.5178
8	*(+) - Coclaurine*	-79.3834	-77.4441
9	*Coreximine*	-81.6152	-74.9462
10	*(-)- Epicatechin*	-75.3858	-72.2675
11	*Isoboldine*	-80.6045	-75.5247
12	*Liriodenine*	-75.857	-70.0643
13	*N-methylcoclaurine*	-86.5039	-75.6987
14	*Remerine*	-81.251	-72.5194
15	*Reticuline*	-85.7013	-77.0767
16	*Palmitic acid*	-88.2824	-80.9118
17	*S-norcorydine*	-75.316	-68.1797
18	*Xylopine*	-79.2331	-69.8403
19	*Cassythicine*	-80.0505	-73.4997
20	*Lysicamin*	-78.0196	-66.8814
21	*(+)- Catechin*	-77.0816	-78.6692
22	*β-sitosterol*	-98.9093	-87.8086
23	*Michelalbine*	-76.3245	-74.2726
24	*Isocorymin*	-68.4169	-71.1142
25	*Nornuciferin*	-76.5729	-70.4907
26	*Ocoteine*	-79.3754	-70.5107
27	*Annomolin*	-128.425	-126.988
28	*cis-annonacin*	-129.145	-122.669
29	*Annomuricin E*	-125.936	-121.313
30	*Quercetin-3-O-glucoside*	-78.5529	-79.7238
31	*Squafosacin-C*	-133.289	-131.825
32	*Muricin A*	-129.741	-124.038
33	*Quercetin*	-72.201	-71.1878

Information:
Docking score of native ligand compound
Docking score of Comparator Drugs
Lower score than Native Ligand and Comparator Drugs

Model of Interaction

The visualization process of interactions between molecules in docking is facilitated by the Biovia Discovery Studio application, which generates representations

of interactions in the form of 2D and 3D images between proteins and test compounds. The results of 2D visualization of potential compounds are also analyzed to identify the amino acid residues involved in each bond. Visualization of potential compounds from the *Annona* genus with target proteins can be seen in **Figures 1** and **Figure 2**. To facilitate analysis of visualization and bond types, **Table 3** provides insight. The visualization results show that the interaction of inhibitors with enzymes occurs in the form of Van der Waals, pi-sigma, conventional hydrogen bonds, carbon-hydrogen bonds, pi-alkyl bonds, and alkyl bonds. The ability of the compound to bind to the target protein is one of the parameters in determining the compound with the most optimal activity.

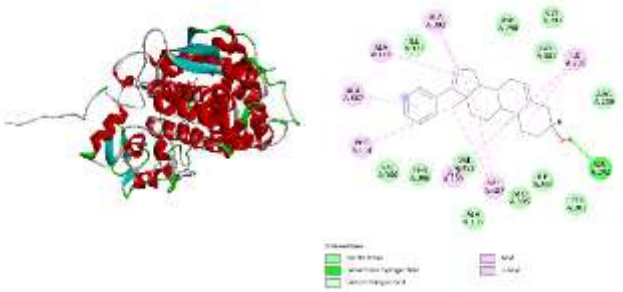

(a)

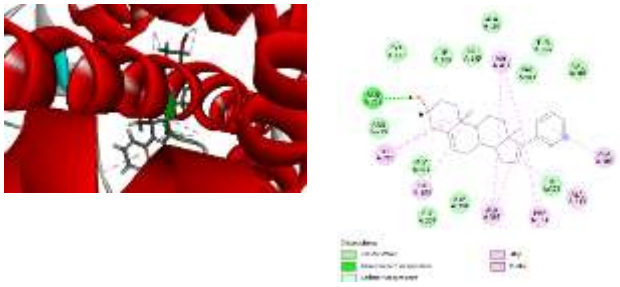

(b)

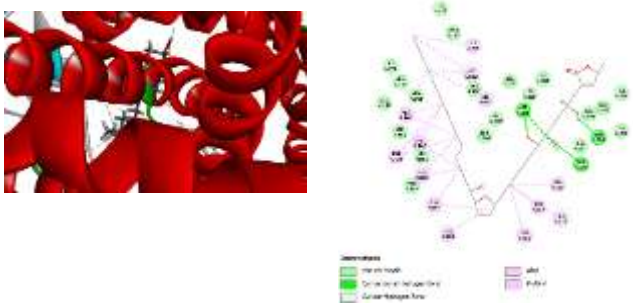

(c)

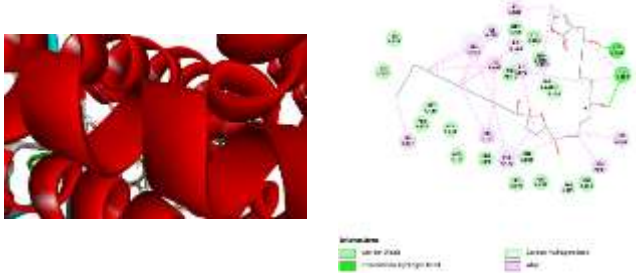

(d)

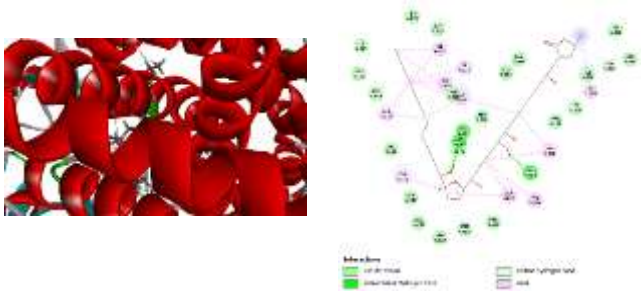

(e)

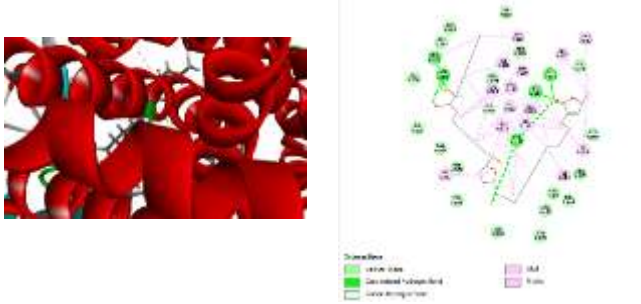

(f)

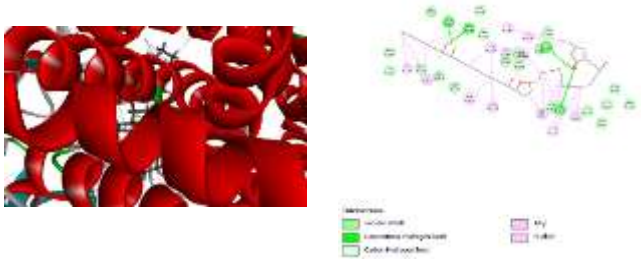

(g)

Figure 1. 3D and 2D interaction visualization of (a) Native Ligand, (b) *Abiraterone*, (c) *Annomolin*, (d) *Cis-annonacin*, (e) *Annomuricin E*, (f) *Squafosacin-C*, and (g) *Muricin A* against 3RUK receptor

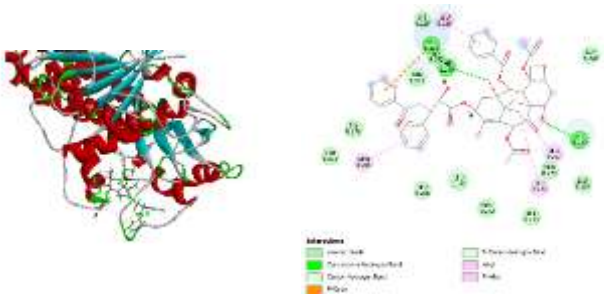

(a)

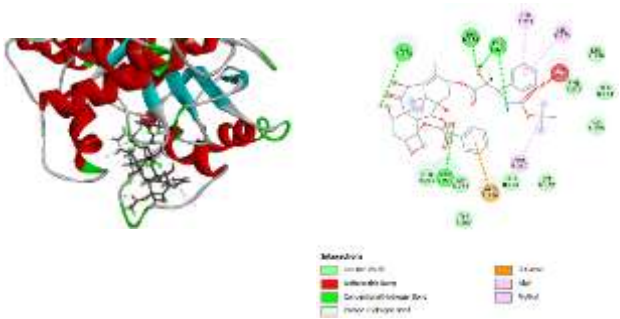

(b)

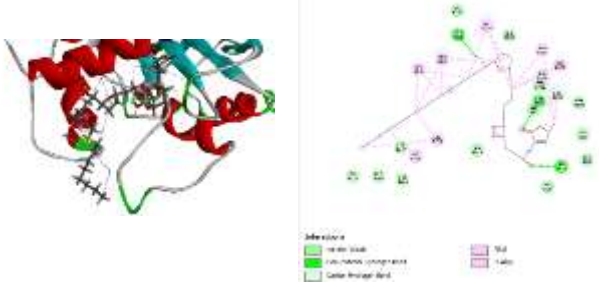

(c)

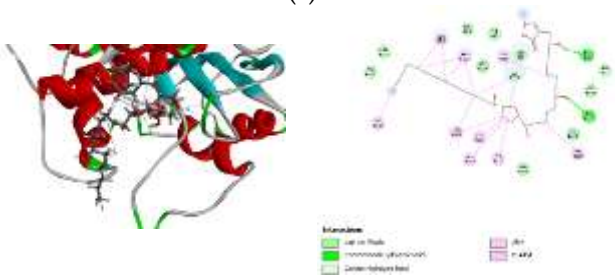

(d)

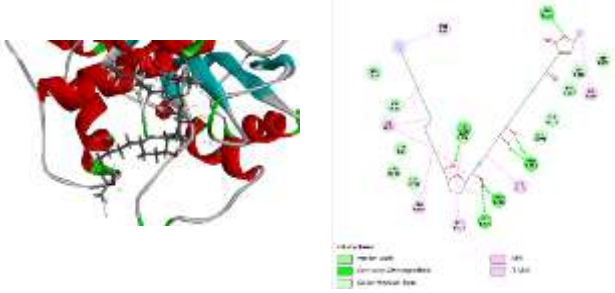

(e)

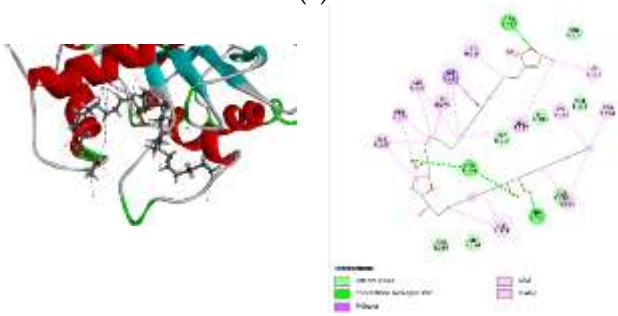

(f)

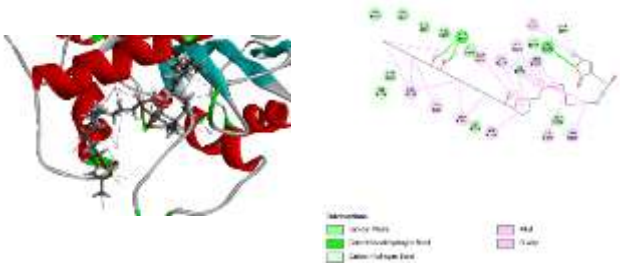

(g)

Figure 2. 3D and 2D interaction visualization of (a) Native Ligand, (b) *Docetaxel*, (c) *Annomolin*, (d) *Cis-annonacin*, (e) *Annomuricin E*, (f) *Squafosacin-C*, and (g) *Muricin A* against 1JFF receptor

Table 3 below lists residues such as ALA A:302, ALA A:367, PHE A:114, ILE A:205, ALA A:113, LEU A:209, VAL A:480, and ASN A:202 that are shared between the native ligand, comparator drug abiraterone, and top Annona compounds. These residues define the active site of CYP17A1, in which steroidal substrates and inhibitors bind. Hydrophobic residues (ALA, ILE, LEU, VAL) line the core of the CYP17A1 active pocket, creating a hydrophobic environment that accommodates the steroidal scaffold of abiraterone and similar molecules. This hydrophobic packing enhances van der Waals stabilization and supports ligand positioning near the heme catalytic center, mirroring findings from recent structural analyses. PHE A:114 engages in π-stacking or hydrophobic contacts with aromatic or non-aromatic rings of steroidal inhibitors, contributing to binding specificity. This residue and surrounding hydrophobic contacts facilitate the tight packing of the ligand into the enzyme's core. ASN A:202 is a key residue that frequently forms direct hydrogen bonds with the C3 keto/hydroxyl group of steroidal inhibitors such as abiraterone, anchoring the ligand in the active site and influencing selectivity and potency. Structural analyses show that this hydrogen bond is conserved across abiraterone and its metabolites bound to CYP17A1. The combination of hydrophobic and hydrogen-bonding interactions in such pockets is a well-recognized principle of steroidogenic enzyme inhibition: the hydrophobic residues provide a complementary surface for steroidal cores, while polar residues such as ASN202 contribute orientation and specificity. Thus, the residue pattern seen in Table 4 is not incidental; these residues form the functionally relevant architecture of the CYP17A1 active site exploited by approved inhibitors such as abiraterone. The conserved interactions of Annona compounds with these residues suggest that they may bind similarly to known inhibitors, with both hydrophobic anchoring and critical hydrogen bonding [29].

The residues identified in **Table 4** below that are shared between the native ligand 1JFF, docetaxel, and the top Annona compounds (e.g., LEU B:217, LEU B:219, HIS B:229, ARG B:284, THR B:278, SER B:277) map directly to the hydrophobic and hydrogen-bonding network within the taxane binding pocket of β-tubulin. This site is critical for tubulin's regulation of polymerization dynamics. Hydrophobic residues such as leucines (e.g., LEU B:217, LEU B:219) line the deeper portion of the taxane pocket and contribute to van der Waals and π-alkyl contacts that stabilize ligands such as docetaxel. This architectural feature suppresses microtubule dynamics, leading to mitotic arrest, a well-established mechanism of taxane chemotherapeutics. The taxane pocket is recognized as a distinct binding site on β-tubulin, exploited by many small-molecule

ligands, in which hydrophobic core residues anchor the bulky, lipophilic moieties of binders [30].

Table 3. Amino acid residue binding similar to Native Ligand in 3RUK protein

Compounds	Amino acid residue interactions							
	ALA A:302	ALA A:367	PHE A:114	ILE A:205	ALA A:113	LEU A:209	VAL A:480	ASN A:202
Native Ligand 3RUK	√	√	√	√	√	√	√	√
Abiraterone (comparator drugs)	√	√	√	√	√	√	√	√
Annomolin	√	√	√		√		√	√
Cis-annonacin	√	√			√		√	
Annomuricin E	√	√		√	√		√	√
Squafosacin-C	√	√	√	√	√	√	√	
Muricin A	√	√	√	√	√			

Interaction description:

Alkyl/pi-alkyl

Conventional hydrogen

Polar and hydrogen bond–forming residues (e.g., HIS B:229, THR B:278, SER B:277) provide additional stabilizing interactions that orient the ligand in a canonical binding pose. HIS229, in particular, has been implicated in stabilizing the ligand network and facilitating correct conformational changes that aid microtubule assembly or disassembly when bound by different modulators [31]. Charged residues such as ARG B:284 can form electrostatic or carbon-hydrogen interactions at the periphery of the pocket, contributing specificity and orientation effects. These conserved interactions explain why both docetaxel and the Annona compounds interact with similar residues: they target the same canonical binding site and thus may modulate tubulin function by overlapping the taxane site's hydrophobic network and hydrogen-bonding framework. Taken together, the pattern of interactions seen in Table 4 shows that the natural products from Annona do not merely bind near tubulin; they engage the same core hydrophobic residues and polar network that characterize clinically relevant taxane-site interactions, an outcome supported by structural studies on tubulin binding sites [30].

Table 4. Amino acid residue binding similar to Native Ligand in 1JFF protein

Compounds	Amino acid residue interactions							
	LEU B:219	ARG B:284	LEU B:217	LEU B:275	HIS B:229	ARG B:278	THR B:276	SER B:277
Native Ligand 1JFF	√	√	√	√	√	√	√	√
Docetaxel (comparator drugs)		√	√	√		√	√	
Annomolin	√			√	√	√		
Cis-annonacin	√		√	√	√			
Annomuricin E					√	√		
Squafosacin-C	√	√	√	√	√	√	√	
Muricin A	√		√	√	√	√		√

Interaction description:

Alkyl/pi-alkyl

Carbon-hydrogen

Conventional hydrogen

In silico interaction analysis was conducted between compounds from the *Annona* genus and amino acid residues of prostate cancer target proteins to evaluate the binding strength of these active compounds. Table 3 and Table 4 presents the similarity of amino acid residue interactions between Annona compounds and control compounds (native ligands and comparator drugs). To facilitate the comparison, similar interacting amino acid residues are highlighted using consistent bold formatting across all compounds. The presence of interactions at the same active site indicates compatibility and alignment of the *Annona* compounds with the binding region, suggesting their potential in inhibiting prostate cancer targets. Compounds predicted to exhibit strong binding are those that form hydrogen bonds with the identical amino acid residues of the receptor protein, as observed in the control compounds.

The bond distance between the ligand and the molecule has an important role in determining the bond, the shorter the bond, the stronger the bond. This also applies to hydrogen bonds, the more hydrogen bonds in the molecule, the more stable the bond [32],[33]. Meanwhile, hydrophobic bonds are bonds formed between the hydrophobic groups of the receptor and the ligand. Hydrophobic bonds support the stability of the complex formed between the receptor and the ligand. The more bonds formed, the more stable the complex will be and the inhibitory activity will also increase [34]. The type of bond that becomes the main parameter in the docking test is the hydrogen bond, because this bond has the highest interaction strength, with energy ranging from 1-7 kcal/mol. In addition, other types of chemical bonds can also be formed due to flexible interactions

between ligands and receptors. Such interactions can be electrostatic bonds (about 5 kcal/mol) and Van der Waals bonds (0.5-1 kcal/mol), which can increase the affinity of the ligand to the receptor, thereby increasing the conformational stability of the ligand-receptor complex [12].

Based on the results of the analysis of amino acid residue similarity in 3RUK and 1JFF receptors, it can be concluded that the number of amino acid residues that interact with ligands plays an important role in determining the position of ligand attachment to proteins. The greater the number of residues involved in the interaction, the higher the affinity or bond strength between the ligand and the target protein [35].

Predicting ADME with Lipinski's Rule of Five

Lipinski's Rule of Five is a reference used to predict the druglikeness, particularly their physicochemical properties, to a high level of oral absorption in the human body. The parameters set in Lipinski's Rule of Five are a partition coefficient (Log P) of ≤ 5, a molecular weight of ≤ 500 g/mol, a hydrogen bond acceptor count of ≤ 10, and a hydrogen bond donor count of ≤5. The Ghose filter is also employed as a rule-based, druggability filter in medicinal chemistry, used to select compound libraries with high drug-likeness, often by identifying molecules likely to be orally bioavailable to ensure small molecules have suitable properties for drug development. It identifies molecules with optimal physicochemical properties, specifically: MW 160–480 g/mol, WlogP −0.4 to 5.6, total atoms 20–70, molar refractivity (MR) 40–130. When a compound meets those principles, it will enhance pharmacokinetic properties and bioavailability during the organism's metabolic process [36],[37].

Table 5. Lipinski's Rule of Five test of potential compounds of the *Annona* genus

Compounds	Molecular weight (g/mol)	H bond donor	H bond acceptor	MLog P	Violation
Native 3RUK	349.51	1	2	4.42	1
Native 1JFF	853.91	4	14	1.70	2
Cis-annonacin	596.88	4	7	3.46	1
Annomolin	596.88	4	7	3.46	1
Annomuricin E	612.88	5	8	2.67	1
Squafosacin-C	580.88	3	6	4.26	1
Muricin A	596.88	4	7	3.46	1

Lipinski's Rule of Five analysis (**Table 5**) was used to assess the oral drug-likeness of the selected Annona compounds. While most Annona derivatives exceed the classical molecular weight threshold of 500 g/mol, they generally satisfy the remaining criteria for hydrogen bond donors, hydrogen bond acceptors, and lipophilicity (MLog P < 5), resulting in only a single rule violation for most compounds. It is now well established that one Lipinski violation does not preclude oral bioavailability, particularly for natural products and enzyme or cytoskeleton-targeting ligands, which often require larger and more flexible scaffolds to engage deep or hydrophobic binding pockets [38],[39].

Importantly, the Annona compounds display moderate lipophilicity (MLog P ≈ 2.6–4.3) and balanced hydrogen-bonding capacity, which are critical determinants of membrane permeability and target engagement. In contrast, the native 1JFF ligand exhibits multiple Lipinski violations, reflecting its poor oral drug-likeness despite high binding affinity. Recent medicinal chemistry studies emphasize that Lipinski's rules should be applied as guidelines rather than strict filters, especially for natural product–

derived leads and anticancer agents targeting complex proteins such as CYP17A1 and β-tubulin [40]. Therefore, although molecular weight remains a potential limitation, the overall physicochemical profiles of the Annona compounds support their consideration as viable lead candidates for further optimization rather than exclusion at the early screening stage.

Table 6. The Ghose filter of potential compounds of the *Annona* genus

Compounds	Molecular weight (g/mol)	Number heavy atoms	WLog P	Molar refractivity	Violation
Native 3RUK	349.51	32	5.40	107.76	0
Native 1JFF	853.91	80	3.41	218.96	3
Cis-annonacin	596.88	42	7.06	172.67	3
Annomolin	596.88	42	7.06	172.67	3
Annomuricin E	612.88	43	6.03	173.84	3
Squafosacin-C	580.88	41	8.09	171.51	3
Muricin A	596.88	42	7.06	172.67	3

Ghose filter analysis (**Table 6**) indicates that the Annona genus compounds fall outside classical drug-like chemical space, primarily due to elevated molecular weight, WLogP, and molar refractivity. However, similar violations are also observed for the native 1JFF ligand, demonstrating that high biological relevance does not necessarily correlate with Ghose compliance. Recent studies emphasize that Ghose criteria are best applied as risk indicators rather than exclusion filters, particularly for natural products and anticancer agents that frequently occupy beyond-rule-of-five space to engage large, hydrophobic protein pockets such as CYP enzymes and microtubules [41],[42]. Therefore, Ghose violations in this study suggest potential pharmacokinetic challenges rather than a lack of therapeutic relevance.

While Lipinski's Rule of Five focuses primarily on oral permeability and hydrogen-bonding balance, the Ghose filter provides a more restrictive assessment of molecular size, polarizability, and lipophilicity. In this study, most Annona compounds exhibit only one Lipinski violation, indicating acceptable drug-likeness at the early screening level. In contrast, Ghose filter analysis reveals multiple violations driven by high molecular weight, WLogP, and molar refractivity. This divergence highlights the complementary nature of the two filters: Lipinski criteria support the feasibility of membrane permeation, whereas Ghose criteria flag increased pharmacokinetic risk associated with structural complexity. Contemporary medicinal chemistry literature recognizes that many approved anticancer drugs and natural product–derived leads intentionally exceed Ghose thresholds to achieve sufficient target engagement within deep hydrophobic cavities, particularly for enzymes such as CYP17A1 and cytoskeletal targets like β-tubulin [41],[43]. Consequently, Ghose filter violations in the present study are interpreted as indicators for future optimization rather than grounds for compound exclusion.

Research Limitation

This study is limited by its reliance on molecular docking, which employs static protein structures and simplified scoring functions reopening binding affinity predictions without fully accounting for protein flexibility, solvent effects, or entropic contributions. In addition, only single crystal structures of CYP17A1 and β-tubulin were used, and molecular dynamics simulations were not performed to evaluate binding

stability over time. Drug-likeness assessments based on Lipinski and Ghose filters provide heuristic guidance but may underestimate the therapeutic potential of natural product–derived compounds that occupy beyond-rule-of-five chemical space. Finally, the absence of experimental validation means that the predicted interactions require confirmation through in vitro and in vivo studies.

4. Conclusion

Based on *in silico* molecular docking analysis, compounds from the Annona genus demonstrate computationally predicted binding potential toward two validated prostate cancer–related targets, CYP17A1 (PDB ID: 3RUK) and β-tubulin (PDB ID: 1JFF). Several Annona-derived compounds exhibited docking scores superior to those of the reference ligands, abiraterone for CYP17A1 and taxol as well as docetaxel for β-tubulin, suggesting favorable theoretical binding affinity. Among these candidates, squafosacin-C showed the strongest predicted interaction with both CYP17A1 (−133.289) and β-tubulin (−131.825) and shared a high degree of binding-site residue similarity with the native ligands, matching 7 of 8 key amino acid residues at both targets. Collectively, these findings indicate that squafosacin-C is a promising lead compound at the computational level, warranting further validation through molecular dynamics simulations and experimental biological assays.

Acknowledgement:

Thanks to the supervisors who contributed to the research and writing of the manuscript, enabling this research to be completed, and the Faculty of Pharmacy University of Borneo Lestari, Banjarbaru.

Conflicts of Interest:

The author declares that there are no conflicts of interest in this research.

References

[1] S. Maekawa, R. Takata, and W. Obara, "Molecular Mechanisms of Prostate Cancer Development in the Precision Medicine Era: A Comprehensive Review," *Cancers (Basel).*, vol. 16, no. 3, pp. 1–34, 2024. [Online]. Available: https://doi.org/10.3390/cancers16030523

[2] N. W. Sangadji and I. M. Ayu, "Modul 13 Epidemiologi Penyakit Kanker Prostat," p. 3, 2018.

[3] E. M. Petrunak et al., "Structures of HumanSteroidogenic CytochromeP45017A1 with Substrates", *Journal of Biological Chemistry*, vol. 289, no. 47, p. e 32952-32964, 2014. [Online]. available: https://doi.org/10.1074/jbc.M114.610998

[4] J. Y. Chuang et al., "Upregulation of CYP17A1 by Sp1-mediated DNA demethylation confers temozolomide resistance through DHEA-mediated protection in glioma", *Oncogenesis*, vol. 6, no. 5, p. e339, 2017. [Online]. available: https://doi.org/10.1038/oncsis.2017.31

[5] J. Puente et al., "Docetaxel in prostate cancer: a familiar face as the new standard in a hormone-sensitive setting," *Therapeutic advances in medical oncology*, vol. 9, no. 5, pp. 307-318, 2017. [Online]. available: https://doi.org/10.1177/1758834017692779

[6] S. Mangaonkar, S. Nath, and B. P. Chatterji, "Microtubule dynamics in cancer metastasis: Harnessing the underappreciated potential for therapeutic interventions," *Pharmacology & therapeutics*, vol. 263, no. 108726, 2024. [Online]. available: https://doi.org/10.1016/j.pharmthera.2024.108726S

[7] Q. H. Chen, "Crosstalk between Microtubule Stabilizing Agents and Prostate Cancer," *Cancers*, vol. 15, no. 13, p. 3308, 2023. [Online]. available: https://doi.org/10.3390/cancers15133308

[8] E. C. McLoughlin and N. M. O'Boyle, "Colchicine-Binding Site Inhibitors from Chemistry to Clinic: A Review," *Pharmaceuticals (Basel, Switzerland)*, vol. 13, no. 1, p. 8, 2020. [Online]. available: https://doi.org/10.3390/ph13010008

[9] S. M. Joseph and A. R. Amala Dev, "Annonaceae: Tropical Medicinal Plants with Potential Anticancer Acetogenins and Alkaloids," in *Bioprospecting of Tropical Medicinal Plants*. K. Arunachalam, X. Yang, and S. P. Sasidharan, Eds. Switzerland: Springer Nature, 2023, pp. 565-578. [Online]. available: https://doi.org/10.1007/978-3-031-28780-0_22

[10] N. Wijayanti, "Review of Docetaxel Interval Usage in Chemotherapy," *J. Surya Med.*, vol. 10, no. 1, pp. 261–264, 2024, [Online]. available: https://doi.org/10.33084/jsm.v10i1.7207

[11] M. Tegar and H. Purnomo, "Tea Leaves Extracted as Anti-Malaria based on Molecular Docking PLANTS," *Procedia Environ. Sci.*, vol. 17, pp. 188–194, 2013, [Online]. available: https://doi.org/10.1016/j.proenv.2013.02.028

[12] H. Ramadhan et al., "In-silico study of antioxidant-anticancer activity of phenolic and flavonoid compounds of Mangifera species using molecular docking PLANTs," *Jurnal Ilmiah Farmasi (Scientific Journal of Pharmacy)*, Special Edition, pp. 8–22, 2023, [Online]. available: https://doi.org/10.20885/jif.specialissue2023.art2.

[13] H. Ramadhan, D. Forestryana, and A. N. Hadi, "Molecular Docking Anti-Melanoma Activity of Compounds from the Alphitonia Genus using PLANTS," *AIP Conf. Proc.*, vol. 3248, no. 1, p. 020018, 2025, [Online]. available: https://doi.org/10.1063/5.0236907/3332003

[14] V. Scardino, M. Bollini, and C. N. Cavasotto, "Combination of pose and rank consensus in docking-based virtual screening: the best of both worlds," *RSC advances*, vol. 11, no. 56, pp. 35383–35391, 2021. [Online]. available: https://doi.org/10.1039/d1ra05785e

[15] F. Ekawasti et al., "Molecular Docking of Red Ginger and Turmeric Compounds on Dense Granules Protein-1 of Toxoplasma gondii Using In Silico Methods," *Jurnal Veteriner*, vol. 22, no. 4, pp. 474–484, 2021, [Online]. available: https://doi.org/10.19087/jveteriner.2021.22.4.474

[16] A. Daina, O. Michielin, and V. Zoete, "SwissADME: a free web tool to evaluate pharmacokinetics, drug-likeness and medicinal chemistry friendliness of small molecules," *Scientific reports*, vol. 7, p. 42717, 2017. [Online]. available: https://doi.org/10.1038/srep42717

[17] S. Forli et al., "Computational protein-ligand docking and virtual drug screening with the AutoDock suite," *Nature protocols*, vol. 11, no. 5, pp. 905–919, 2016. [Online]. available: https://doi.org/10.1038/nprot.2016.051

[18] X. Y. Meng et al., "Molecular docking: a powerful approach for structure-based drug discovery," *Current computer-aided drug design*, vol. 7, no. 2, pp. 146–157, 2011. [Online]. available: https://doi.org/10.2174/157340911795677602

[19] T. Pantsar and A. Poso, "Binding Affinity via Docking: Fact and Fiction," *Molecules (Basel, Switzerland)*, vol. 23, no. 8, p. 1899, 2018. [Online]. available: https://doi.org/10.3390/molecules23081899

[20] N. S. Pagadala, K. Syed, and J. Tuszynski, "Software for molecular docking: a review," *Biophysical reviews*, vol. 9, no. 2, pp. 91–102, 2017. [Online]. available:

https://doi.org/10.1007/s12551-016-0247-1

[21] J. Uppal and R. Sharma, "Current advancements in tubulin targeting agents for breast cancer: Design strategies, structure-activity relationships, and pharmacological insights," *Biochemical and biophysical research communications*, vol. 793, p. 153019, 2025. [Online]. available: https://doi.org/10.1016/j.bbrc.2025.153019

[22] Z. Ma, A. Ajibade, and X. Zou, "Docking strategies for predicting protein-ligand interactions and their application to structure-based drug design," *Communications in information and systems*, vol. 24, no. 3, pp. 199–230, 2024. [Online]. available: https://doi.org/10.4310/cis.241021221101

[23] M. Y. Alsedfy et al., "Investigating the binding affinity, molecular dynamics, and ADMET properties of curcumin-IONPs as a mucoadhesive bioavailable oral treatment for iron deficiency anemia," *Scientific reports*, vol. 14, no. 1, p. 22027, 2024. [Online]. available: https://doi.org/10.1038/s41598-024-72577-8

[24] A.A. Mohamed Yusoff et al., "Somatic mitochondrial DNA D - loop mutations in meningioma discovered : A preliminary data," *J. Cancer Res. Ther.*, vol. 16, no. 6, pp. 1517–1521, 2020. [Online]. available: https://doi.org/10.4103/jcrt.JCRT_1132_16

[25] P. Binarová and J. Tuszynski, "Tubulin: Structure, functions and roles in disease," *Cells*, vol. 8, no. 10, p. 1294, 2019, [Online]. available: https://doi.org/10.3390/cells8101294

[26] S. A. H. Abdi et al., "Morusflavone, a New Therapeutic Candidate for Prostate Cancer by CYP17A1 Inhibition: Exhibited by Molecular Docking and Dynamics Simulation," *Plants (Basel, Switzerland)*, vol. 10, no. 9, p. 1912, 2021. [Online]. available: https://doi.org/10.3390/plants10091912

[27] S. A. Dhawale et al., "In silico screening and molecular mechanics analysis of phytocompounds obtained from genus Diospyros as potential CYP17A1 inhibitors for prostate cancer therapy," *In Silico Research in Biomedicine*, vol. 1, p. 100130, 2025. [Online]. available: https://doi.org/10.1016/j.insi.2025.100130

[28] D. Bora et al., "Exploration of cytotoxic potential and tubulin polymerization inhibition activity of cis-stilbene-1,2,3-triazole congeners," *RSC medicinal chemistry*, vol. 14, no. 3, pp. 482–490, 2023. [Online]. available: https://doi.org/10.1039/d2md00400c

[29] E. M. Petrunak et al., "Human cytochrome P450 17A1 structures with metabolites of prostate cancer drug abiraterone reveal substrate-binding plasticity and a second binding site," *The Journal of biological chemistry*, vol. 299, no. 3, p. 102999, 2023. [Online]. available: https://doi.org/10.1016/j.jbc.2023.102999

[30] M. Ezzo and S. Etienne-Manneville, "Microtubule-Targeting Agents: Advances in Tubulin Binding and Small Molecule Therapy for Gliomas and Neurodegenerative Diseases," *International journal of molecular sciences*, vol. 26, no. 15, p. 7652, 2025. [Online]. available: https://doi.org/10.3390/ijms26157652

[31] F. d. A. Balaguer et al., "Crystal Structure of the Cyclostreptin-Tubulin Adduct: Implications for Tubulin Activation by Taxane-Site Ligands," *International Journal of Molecular Sciences*, vol. 20, no. 6, p. 1392, 2019. [Online]. available: https://doi.org/10.3390/ijms20061392

[32] Q. X. A. Kai et al., "Molecular docking of marine fauna glutathion towards receptors of several viral diseases," *Jurnal Pesisir dan Laut Tropis*, vol. 9, no. 2, pp. 53-58, 2021. [Online]. available: https://doi.org/10.35800/jplt.9.2.2021.34853

[33] I. K. Kenyori, M. S. Alamsyah, and C. I. A. Nurjanah, "In Silico Study of The

Quercetin Bioactive Compound of Lime Peel (*Citrus aurantifolia*) as Anti Breast Cancer Agent," *B I M F I*, vol. 9, no. 1, pp. 1–10, 2022. [Online]. available: https://doi.org/10.48177/bimfi.v9i1.95

[34] A. M. Sururi, D. K. Maharani, and F. A. Wati, "Potency of Eugenol Compounds from Clove (*Syzygium Aromaticum*) as HIV-1 Protease (PR) Inhibitors," *Unesa Journal of Chemistry*, vol. 12, no. 1, pp. 26–30, 2023, [Online]. available: https://doi.org/10.26740/ujc.v12n1.p26-30

[35] F. Z. Muttaqin, "Molecular Docking and Molecular Dynamic Studies of Stilbene Derivative Compounds As Sirtuin-3 (Sirt3) Histone Deacetylase Inhibitor on Melanoma Skin Cancer and Their Toxicities Prediction," *Journal of Pharmacopolium*, vol. 2, no. 2, pp. 112–121, 2019. [Online]. available: https://doi.org/10.36465/jop.v2i2.489

[36] A. R. Dewayani *et al.*, "In Silico Study of Soursop Leaf Compounds (Annona muricata L.) as Inhibitors of BRAF V600E in Melanoma Cancer," *Jurnal Farmasi Udayana*, vol. 11, no. 2, pp. 80-88, 2023. [Online]. available: https://doi.org/10.24843/JFU.2022.v11.i02.p07

[37] M. Rai et al., "Herbal concoction Unveiled: A computational analysis of phytochemicals' pharmacokinetic and toxicological profiles using novel approach methodologies (NAMs)," *Current research in toxicology*, vol. 5, p. 100118, 2023. [Online]. available: https://doi.org/10.1016/j.crtox.2023.100118

[38] B. C. Doak and J. Kihlberg, "Drug discovery beyond the rule of 5 - Opportunities and challenges," *Expert opinion on drug discovery*, vol. 12, no. 2, pp. 115–119, 2017. [Online]. available: https://doi.org/10.1080/17460441.2017.1264385

[39] S. Lindner et al., "Strategies to Improve the Lipophilicity of Hydrophilic Macromolecular Drugs," *Advanced healthcare materials*, vol. 15, no. 5, p. e03721, 2026. [Online]. available: https://doi.org/10.1002/adhm.202503721

[40] R. Ancuceanu et al., "In Silico ADME Methods Used in the Evaluation of Natural Products," *Pharmaceutics*, vol. 17, no. 8, p. 1002, 2025. [Online]. available: https://doi.org/10.3390/pharmaceutics17081002

[41] S. Kralj, M. Jukič, and U. Bren, "Molecular Filters in Medicinal Chemistry," *Encyclopedia*, vol. 3, no. 2, pp. 501-511, 2023. [Online]. available: https://doi.org/10.3390/encyclopedia3020035

[42] S. Senese et al., "Microtubins: a novel class of small synthetic microtubule targeting drugs that inhibit cancer cell proliferation," *Oncotarget*, vol. 8, no. 61, pp. 104007–104021, 2017. [Online]. available: https://doi.org/10.18632/oncotarget.21945

[43] D. J. Newman and G. M. Cragg, "Natural products as sources of new drugs: recent trends," *Journal of Natural Products*, vol. 83, no. 3, pp. 770–803, 2020. [Online]. available: https://doi.org/10.1021/acs.jnatprod.9b01285